Robotica (1999) volume 17, pp. 513–521. Printed in the United Kingdom © 1999 Cambridge University Press

Swing-free transportation of suspended objects with robot manipulators

Gürsel Alıcı, Sadettin Kapucu and Sedat Bayseç

Gaziantep University, Faculty of Engineering, Department of Mechanical Engineering, TR-27310 Gaziantep (Turkey)
E-mail: gursel@alpha.bim.gantep.edu.tr

(Received in Final Form: March 20, 1999)

SUMMARY

This paper addresses the swing-free transport of simply suspended objects which cannot be grasped by robot manipulators, and therefore, must be carried by a hook or a similar device attached to the manipulator endpoint. Two methods are presented to stop the suspended object in a swing-free state at the end of a move/gross motion; (1) limiting transportation time, thus stopping the manipulator at the instant when the object completes one or more full cycle(s), and (2) adjusting traveling time of each section of a three-piece continuous trajectory provided that a given transportation time is unchanged. A hydraulically actuated robot manipulator carrying a compound pendulum was employed as an experimental system to test the methods. Simulation and experimental results are presented to demonstrate the feasibility of both methods. It is concluded that while limiting transportation time is not a preferred way to eliminate swing at the end of the move as it depends on the period of oscillation of the suspended object, the latter is a more practical and applicable method and is valid for moves of any length. The results reveal that by properly planning the acceleration of the transporting device, a robot manipulator or a similar device such as a crane, a swing-free stop is obtainable. The proposed approaches are simple and easy to implement.

KEYWORDS: Suspended objects; Swing-free transportation; Motion design; Acceleration planning; Robots; Crane.

1. INTRODUCTION

In most robotic applications, the load carried by a robot manipulator is held firmly and not allowed to move relative to the gripper. In such a case, the load may be assumed to be a part of the last link. Many researchers consider the load like this and assume it to do the same motion as the last link of the manipulator. But, in some cases, the load may be able to move or swing, and thus displays a motion separate from the manipulator. Such applications can be typified by an object suspended from the manipulator end point via a hook-like device,[1] the transport of large objects in a factory environment by the use of a bridge crane by which the object is raised, transported and lowered on a target location,[2] and a molten-metal filled container carried by a manipulator in a foundry where the molten-metal should not splash at the end of the transportation where pouring the metal into the molds takes place. The transport of such objects generally result in undesired swing at the end of a move.

In order to stop a suspended object in a swing-free state, Starr,[1] has suggested a trajectory consisting of an acceleration part, where the suspension point is accelerated stepwise until half the desired transportation velocity is reached and then is further stepwise accelerated to the specified final velocity which is attained at a point roughly at one-fourth of the transportation velocity times the period of natural oscillation of the suspended object, and a deceleration part, where the same process is applied in reverse. Later, Strip,[2] has reported on the swing-free transportation of suspended objects that the suspension point begins to be decelerated at the same rate as it is accelerated, starting at a distance from its goal equal to the distance travelled while accelerating. This distance is reported to be one-half the acceleration of the suspension point times the square of the natural period of oscillation of the object.

In this study, two methods are presented to eliminate swing at the end of any move provided that the transportation device has zero initial and final velocities and accelerations, based on choosing an appropriate trajectory for the suspension point. Trajectories employed are different than those reported before.[1–5] It is therefore believed that this study contributes to the efforts to eliminate swinging of suspended objects. We assume that the compliance existing in the transmission and structural elements does not cause considerable vibration of the manipulator endpoint during and at the end of the move, and the suspension point follows a pre-determined path with a certain velocity and acceleration. This is verified by the experimental results presented in Section 4, the prismatic joint following a commanded trajectory without any vibration. Employing a preshaped desired input strengthens this assumption.[3,4,6] To demonstrate the feasibility of both methods, we consider two trajectories based on a cycloidal motion which is commonly used as a high-speed cam profile, continuous throughout one cycle. This does not introduce any high frequency inputs to the system and hence reduces unwanted dynamic effects. A full cycloid is proposed for the first method, and a three-piece trajectory which consists of a half cycle accelerating cycloid, a ramp (a constant velocity) and a half cycle decelerating cycloid for the second. Note that both trajectories for the transportation device are continuous to the first order. Any other trajectory which has no abrupt

https://doi.org/10.1017/S0263574799001666 Published online by Cambridge University Press

changes in position, velocity and acceleration from the beginning to the end of the motion also can be employed.

This study proves that the method of limiting transportation time restricts the transportation time to the period of natural oscillations of the suspended object and is not a versatile method. On the other hand, the method of using a three-piece trajectory is valid for moves of any length and is a versatile method to prevent swing at the end of a move. Note that the traveling time for each piece of the three-piece continuous trajectory are adjusted such that a given transportation time and continuity of velocities at the junctions are satisfied, and there is no swing at the end of the move. As given in section 3.2, the traveling times for the accelerating and decelerating eras are selected in order to prevent accelerations and decelerations out of the capability of the transporting device, and the traveling time for the constant velocity or zero acceleration era are calculated. An object suspended at the end of a robot manipulator by a hook-like device is considered and its equation of motion is solved on a digital computer for the acceleration profile of the suspension point. Simulation results have been verified on a hydraulically actuated robot manipulator whose translational link carrying a compound pendulum. Simulation and experimental results reveal that both methods are applicable and easy to implement on a real system.

2. MODELLING AND ANALYSIS OF SUSPENDED OBJECT

Consider an object suspended from the end of a robot manipulator by a hook, as depicted in Figure 1, where "O" is the point of suspension, "**x**" is the horizontal displacement of point "O", θ is the angular displacement of the object with the vertical, **m** is the mass of the object, $\mathbf{I_G}$ is the mass moment of inertia about the center of gravity of the object, **r** is the radial distance from the center of gravity to the point of suspension "O". We assume that the manipulator endpoint moves and accelerates in one direction, say in **x** direction. The mathematical model of the suspended object can be derived by employing Lagrangian equation defined as follows[7]

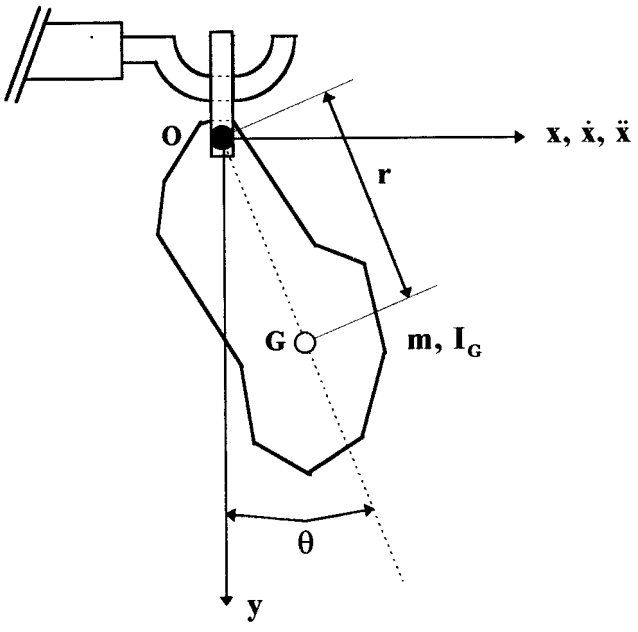

Fig. 1. An object suspended from a manipulator endpoint via a hook.

$$\frac{\mathbf{d}}{\mathbf{dt}}\left(\frac{\partial \mathbf{L}}{\partial \dot{\mathbf{q}}_\mathbf{i}}\right)-\frac{\partial \mathbf{L}}{\partial \mathbf{q_i}}=\mathbf{F_i},\quad \mathbf{i=1,\ 2,\ 3,\ .....n} \tag{1}$$

where **L** is the Lagrangian defined as $\mathbf{L=T-V}$, **T** and **V** denote respectively, the total kinetic energy and the total potential energy of the system, $\mathbf{q_i}$ represents the set of generalised coordinates, and $\mathbf{F_i}$ is the generalised force acting along the **i-th** generalised coordinate. For this work, there are no generalised forces $\mathbf{F_i}$ explicitly acting on the object and the generalised coordinate is the angle θ made by the axis of symmetry of the object with the vertical.

The total kinetic energy of the suspended object with mass **m** and mass moment of inertia $\mathbf{I_G}$ is;

$$\mathbf{T}=\frac{1}{2}\mathbf{mV_G^2}+\frac{1}{2}\mathbf{I_G}\dot{\theta}^2=\frac{1}{2}\mathbf{m}(\dot{\mathbf{x}}^2+\mathbf{r}^2\dot{\theta}^2+2\mathbf{r}\dot{\mathbf{x}}\dot{\theta}\ \mathbf{cos}\ \theta)+\frac{1}{2}\mathbf{I_G}\dot{\theta}^2 \tag{2}$$

where $\mathbf{v_G}$ is the linear absolute velocity of the mass center of the object, and $\dot{\theta}$ is the time derivative of the angle θ. The gravitational potential energy of the suspended object with respect to the resting position of the mass center is;

$$\mathbf{V=mgr(1-cos\theta)} \tag{3}$$

Employing Lagrange formulation defined by Eq. 1 for the generalised coordinate θ gives the following differential equation of motion;

$$\ddot{\theta}+\frac{\mathbf{mgr}}{\mathbf{I_o}}\mathbf{sin}\,\theta=-\frac{\mathbf{mr}}{\mathbf{I_o}}\ddot{\mathbf{x}}\mathbf{cos}\,\theta,\ \text{where}\ \mathbf{I_o=I_G+mr^2} \tag{4}$$

Eq. 4 is a nonlinear differential equation which can be linearised by substituting $\mathbf{sin}\ \theta=\theta$ and $\mathbf{cos}\ \theta=\mathbf{1}$ into Eq. 4 with an error less than **1%**, if $\theta<\mathbf{5.5°}$ of its motion.[8] Eq. 4, then becomes:

$$\ddot{\theta}+\omega_n^2\theta=\mathbf{K}\ddot{\mathbf{x}},\ \text{where}\ \omega_n^2=\frac{\mathbf{mgr}}{\mathbf{I_o}},\ \mathbf{K}=-\frac{\omega_n}{\mathbf{g}} \tag{5}$$

ω_n being the natural frequency, note that the motion of the suspended object is a simple-periodic motion while the point of suspension "O" is accelerating with $\ddot{\mathbf{x}}$ which is the forcing function exciting the suspended object. Depending on the form of $\ddot{\mathbf{x}}$, the solution for Eq. 5 is obtained.

3. ELIMINATION OF SWING

The acceleration profile for the suspension point "O" is assumed to be known and can be mathematically defined. The acceleration trajectory of a full cycloid, and a three-piece trajectory are employed for the first and the second approaches, respectively.

3.1 Limiting Transportation Time

A full cycloidal motion profile for the pre-determined path of the suspension point which has continuous derivatives at

https://doi.org/10.1017/S0263574799001666 Published online by Cambridge University Press

the beginning and at the end of a move is expressed as;

$$x = \frac{X}{2\pi}\left[\frac{2\pi t}{\tau} - \sin 2\pi\frac{t}{\tau}\right] \tag{6}$$

where **X** is the total distance to be travelled, **t** is time into motion, and τ is the total traveling time. So, the corresponding acceleration profile is;

$$\ddot{x} = R \sin \omega t \quad \text{where } R = \frac{2\pi X}{\tau^2}, \quad \omega = \frac{2\pi}{\tau} \tag{7}$$

This acceleration profile is employed to demonstrate the feasibility of the method of limiting traveling time to eliminate swing. Any other end point trajectory which has no abrupt changes in position, velocity and acceleration from the beginning to the end of the motion can be similarly employed.

The solution of Eq. 5 under the acceleration profile defined by Eq. 7 for zero initial conditions is

$$\theta(t) = \frac{KR}{\omega_n^2 - \omega^2}\left[\sin\omega t - \frac{\omega}{\omega_n}\sin\omega_n t\right]$$

$$= D\left[\sin\omega t - \frac{\omega}{\omega_n}\sin\omega_n t\right] \tag{8}$$

This solution is valid until $t = \tau$. After that time, $\ddot{x} = 0$, and the solution of Eq. 5 becomes;

$$\theta = A \sin \omega_n(t-\tau) + B \cos \omega_n(t-\tau) \tag{9}$$

The arbitrary constants **A** and **B** are evaluated from the final value of Eq. 8 and its time derivative at $t = \tau$. They are found as

$$\frac{A = D\frac{\omega}{\omega_n}(\cos\omega\tau - \cos\omega_n\tau)}{B = D\left(\sin\omega\tau - \frac{\omega}{\omega_n}\sin\omega_n\tau\right)} \tag{10}$$

It is essential to set **A** and **B** to zero simultaneously to have no swing after $t > \tau$. This yields the following solution for the total traveling time τ;

$$\tau = \frac{n2\pi}{\omega_n} = n2\pi\sqrt{\frac{I_o}{mgr}}, \quad n = 2, 3, 4 \ldots\ldots \tag{11}$$

Note that Eq. 11 gives the second and higher harmonics of the natural period of oscillation of the suspended object. The differential equation of motion of the suspended object is solved on a digital computer for the cycloidal motion profile for the given duration determined from Eq. 11, using the MATLAB function "ode45" based on fourth and fifth-order Runge-Kutta numerical integration algorithms.[9] The period of oscillation of the compound pendulum considered is taken as **1.4** seconds or the natural frequency **4.4867 rad/sec**. The distance **X** to be covered is arbitrarily taken as 0.292 m in the simulation. The same data is used in Section 4 for experimental verification. The simulation result is depicted in Figure 2. Note that there is no swing when $t > \tau$. When the duration is provided without considering Eq. 11, the suspended object keeps swinging at the end of the move, as seen in Figure 3.

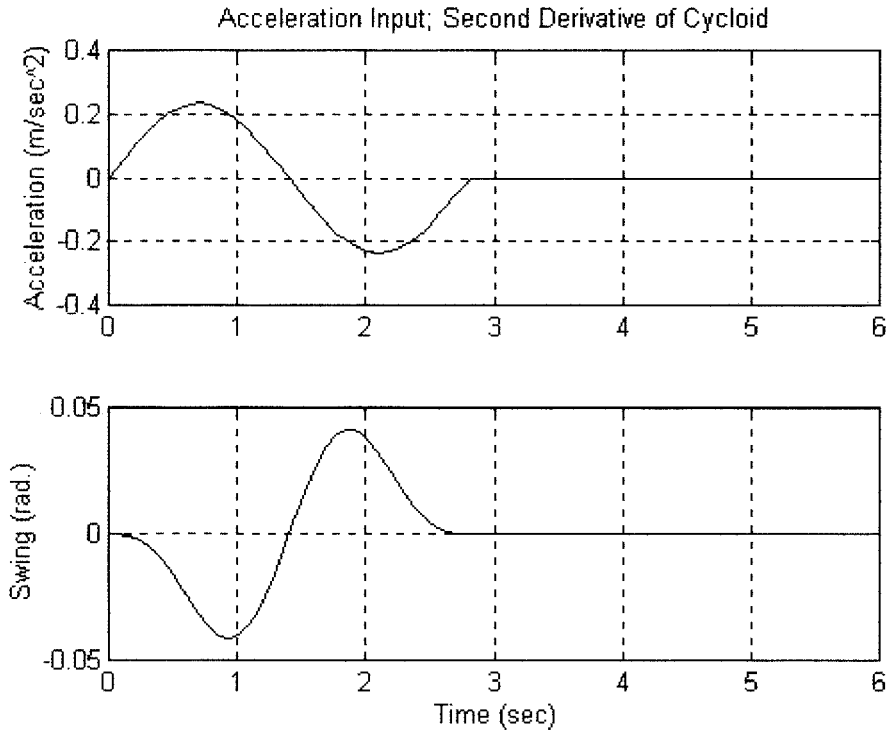

Fig. 2. Swing-free response of the suspended object for n = 2.

https://doi.org/10.1017/S0263574799001666 Published online by Cambridge University Press

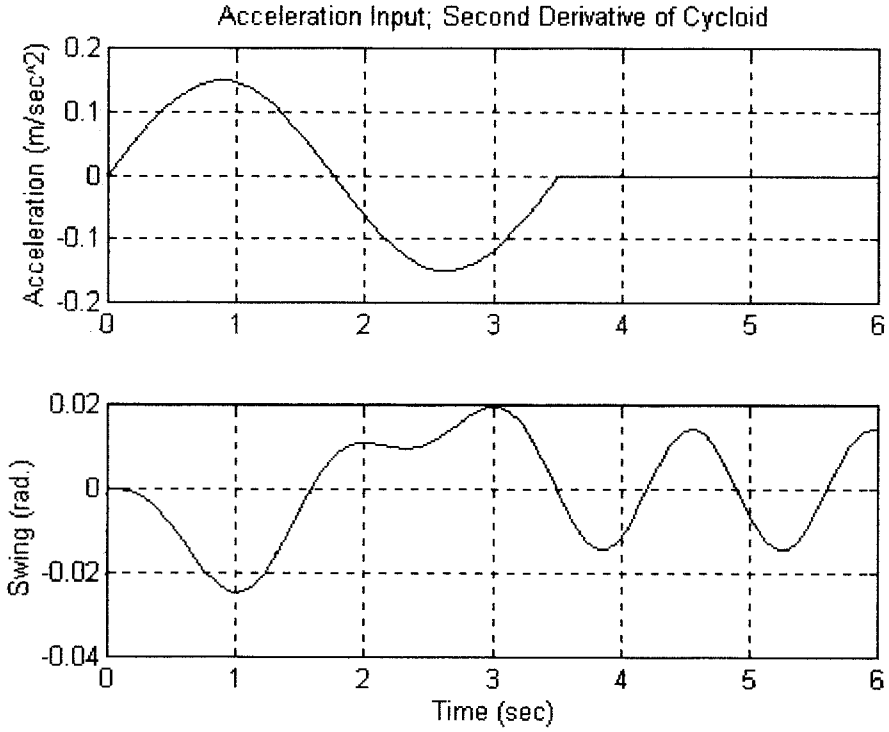

Fig. 3. Swinging response of the suspended object for n = 2.5.

3.2 Adjusting Traveling Time for Each Piece of a Three-piece Trajectory

Rather than accelerating and then decelerating the transportation device consecutively, it might be advantageous to have a constant velocity period after an acceleration period, and then a deceleration period in order to stop at the end of any desired distance. A trajectory consisting of a half cycloid accelerating, a ramp (constant velocity) and another half cycloid decelerating, which is depicted in Figure 4, is employed to satisfy those requirements. This is widely used in the design of cam contours.[10] The swing generated by a dynamic load at the end of the move can be eliminated by adjusting the traveling duration for each profile, as in that of the follower of a cam mechanism.

The problem set forth now is to determine the amplitude and the duration of each half cycloid motion segment such that the total distance covered is the desired distance of travel and the total time elapsing is equal to the traveling

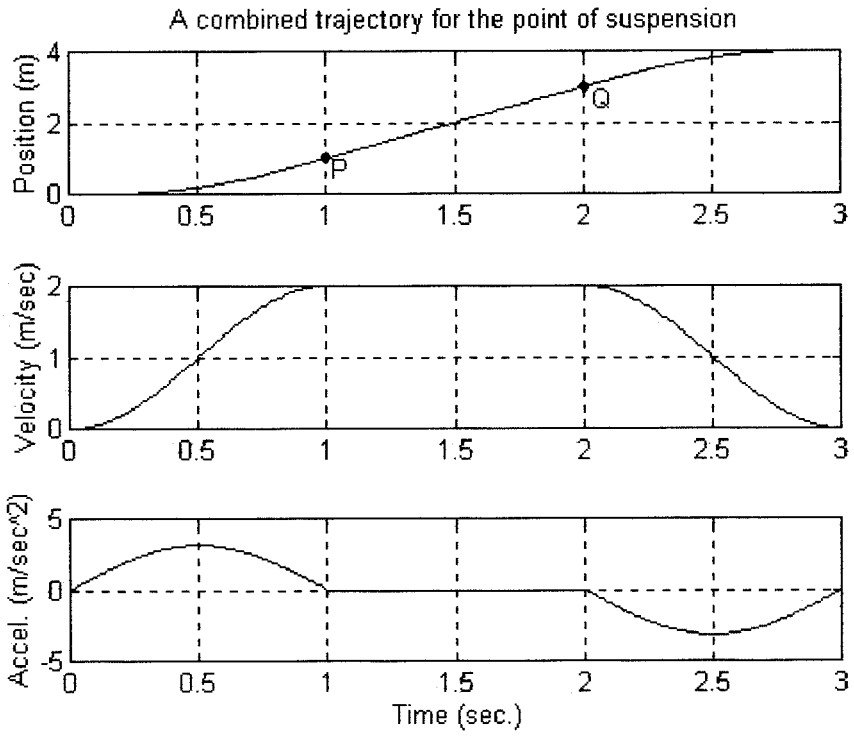

Fig. 4. A trejectory consisting of a cycloid, a constant velocity, and a cycloid.

https://doi.org/10.1017/S0263574799001666 Published online by Cambridge University Press

time. Also, the velocities of all profiles at the junction must be equal. This provides a first order continuity in the motion of the transporting device. For high speed applications, a second order continuity may be sought for by using double harmonic motion profiles. Each part of the three-piece trajectory and their second time derivatives are given as

$$x_1 = X_1\left[\frac{t}{\tau_1} - \frac{1}{\pi}\sin\pi\frac{t}{\tau_1}\right], \quad \ddot{x}_1 = \frac{\pi X_1}{\tau_1^2}\sin\frac{\pi}{\tau_1}t = R_1\sin\omega_1 t$$

$$x_2 = \frac{X_2}{\tau_2}t, \quad \ddot{x}_2 = 0, \tag{12}$$

$$x_3 = X_3\left[\frac{t}{\tau_3} + \frac{1}{\pi}\sin\pi\frac{t}{\tau_3}\right],$$

$$\ddot{x}_3 = -\frac{\pi X_3}{\tau_3^2}\sin\frac{\pi}{\tau_3}t = -R_3\sin\omega_3 t,$$

where X_1, X_2, X_3 are the distances covered and τ_1, τ_2, τ_3, are the elapsing times for the first, second and the third motion segments, respectively, hence

$X = X_1 + X_2 + X_3$ and $\tau = \tau_1 + \tau_2 + \tau_3$,

$$R_1 = \frac{\pi X_1}{\tau_{1_1}^2}, \quad \omega_1 = \frac{\pi}{\tau_1}, \quad R_3 = \frac{\pi X_3}{\tau_{3_1}^2}, \omega_3 = \frac{\pi}{\tau_3}.$$

A velocity match at the junction **P** and **Q** require, respectively

$$\frac{2X_1}{X_2} = \frac{\tau_1}{\tau_2} \quad \text{and} \quad \frac{X_1}{X_3} = \frac{\tau_1}{\tau_3} \tag{13}$$

We assume that the traveling time τ_1 and τ_3 are equal to each other and therefore X_1 and X_3 distances covered in, the accelerating and decelerating parts are also equal. They are to be specified according to the acceleration and deceleration capability and the maximum available velocity of the transporting device. So, the traveling time for the constant velocity trajectory and its amplitude are evaluated from the conditions of zero swing at the end of the move and the proper velocity match at the junctions P and Q.

Since Eq. 5 is a linear differential equation, it can be solved consecutively for three forcing functions between the specified time intervals. For zero initial conditions and the interval of $0 \le t \le \tau_1$, the solution for the differential equation given by Eq. 5 is

$$\theta_1(t) = \frac{KR_1}{\omega_n^2 - \omega_1^2}\left[\sin\omega_1 t - \frac{\omega_1}{\omega_n}\sin\omega_n t\right]$$

$$= D_1\left[\sin\omega_1 t - \frac{\omega_1}{\omega_n}\sin\omega_n t\right] \tag{14}$$

For the interval of $\tau_1 \le t \le (\tau_1 + \tau_2)$, where $\ddot{x}$ of Eq. 5 is $\ddot{x}_2$, it is;

$$\theta_2(t) = A_2\sin\omega_n(t - \tau_1) + B_2\cos\omega_n(t - \tau_1) \tag{15}$$

where

$$A_2 = -D_1\frac{\omega_1}{\omega_n}[1 + \cos\omega_n\tau_1], \quad B_2 = -D_1\frac{\omega_1}{\omega_n}\sin\omega_n\tau_1$$

For the interval of $(\tau_1 + \tau_2) \le t \le (\tau_1 + \tau_2 + \tau_3)$, where $\ddot{x}$ of Eq. 5 is $\ddot{x}_3$, it is;

$$\theta_3(t) = A_3\sin\omega_n(t - \tau_1 - \tau_2) + B_3\cos\omega_n(t - \tau_1 - \tau_2) - \frac{KR_3}{\omega_n^2 - \omega_3^2}\sin\omega_3(t - \tau_1 - \tau_2) \tag{16}$$

where

$$B_3 = \theta_2(\tau_2), \quad A_3 = \frac{\dot{\theta}_2(\tau_2) + D_3}{\omega_n}, \quad D_3 = \frac{KR_3\omega_3}{\omega_n^2 - \omega_3^2}$$

For the interval of $t > (\tau_1 + \tau_2 + \tau_3)$, where $\ddot{x}$ of Eq. 5 is zero, it is;

$$\theta_4(t) = A_4\sin\omega_n(t - \tau) + B_4\cos\omega_n(t - \tau) \tag{17}$$

where

$$B_4 = \theta_3(\tau_3), \quad A_4 = \frac{\dot{\theta}_3(\tau_3)}{\omega_n}$$

It is essential to set A_4 and B_4 to zero simultaneously to have no swing after $t > \tau$. As mentioned before, the traveling duration and amplitudes for the accelerating and decelerating sections are provided to prevent a possibility of requiring accelerations and decelerations out of the capability of the manipulator. The only unknown is then the constant velocity duration τ_2. It is evaluated such that the total duration and the total amplitude are the desired traveling time and the desired distance. τ_2 explicitly appears in A_3 and B_3 of Eq. 16 from which,

$$B_3 = A_2\sin\omega_n\tau_2 + B_2\cos\omega_n\tau_2$$
$$A_3 - \frac{D_3}{\omega_n} = A_2\cos\omega_n\tau_2 - B_2\sin\omega_n t_2 \tag{18}$$

A_3 and B_3 are calculated from Eq. 17 by equating A_4 and B_4 to zero. A_2 and B_2 are obtained from Eq. 15. Note that Eq. 18 consists of two nonlinear-trigonometric equations, and they are converted into simultaneous nonlinear polynomial equations by using tangent half-angle identities;

$$(B_2 + B_3)s^2 - 2A_2 s + (B_3 - B_2) = 0$$
$$\left(A_3 - \frac{D_3}{\omega_n} + A_2\right)s^2 + 2B_2 s + \left(A_3 - \frac{D_3}{\omega_n} - A_2\right) = 0 \tag{19}$$

where

$$s = \tan\left(\frac{\omega_n\tau_2}{2}\right)$$

To give an example, Eq. 19 is simultaneously solved for $\tau_1 = \tau_3 = 1.2$ seconds, $X_1 = X_3 = 0.125$ meters and $\omega_n = 4.4867$ **rad/sec**. The unknown τ_2 is calculated as 0.200 second, and the corresponding amplitude X_2 is determined by employing

https://doi.org/10.1017/S0263574799001666 Published online by Cambridge University Press

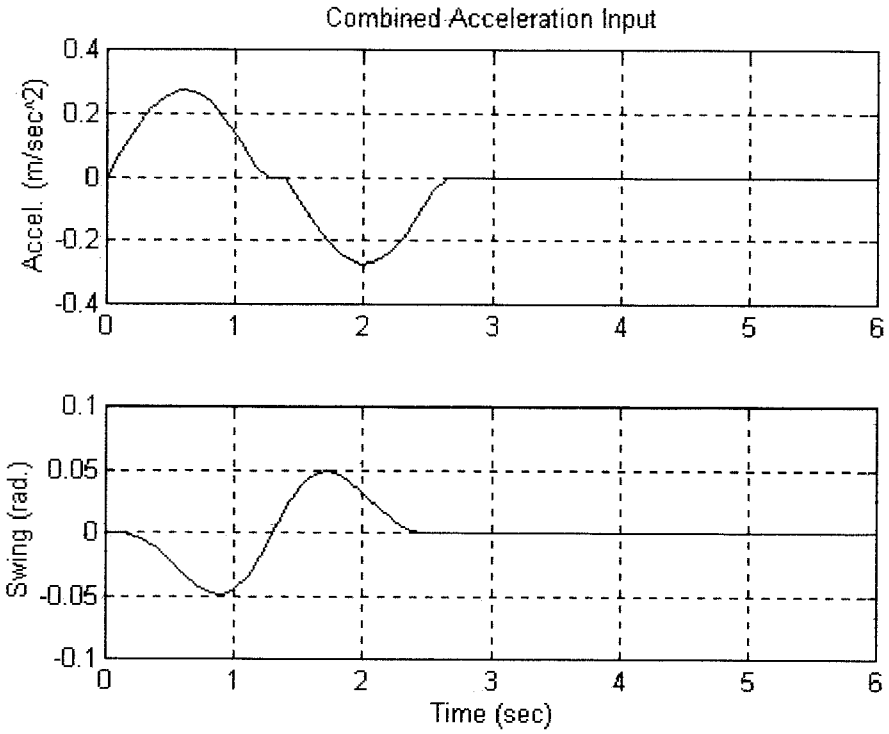

Fig. 5. Swing-free response of the suspended object.

Eq. 13. Consequently, it is possible to have solutions satisfying Eq. 19 simultaneously. Then by using the specified and the calculated quantities, the differential equation of motion given by Eq. 5 is solved on a digital computer for each of the forcing functions again using the MATLAB function "ode45". The solution obtained is depicted in Figure 5, where it is clearly seen that there is no swing when $\mathbf{t} > (\tau_1 + \tau_2 + \tau_3)$. When the duration for each part is provided without considering the approach presented above, the suspended object keeps swinging at the end of the move, as seen in Figure 6.

4. Experimental Verification

The experimental set-up is shown in Figure 7. Key elements of the set-up are a hydraulically actuated manipulator of Stanford type, a compound pendulum attached to the tip of

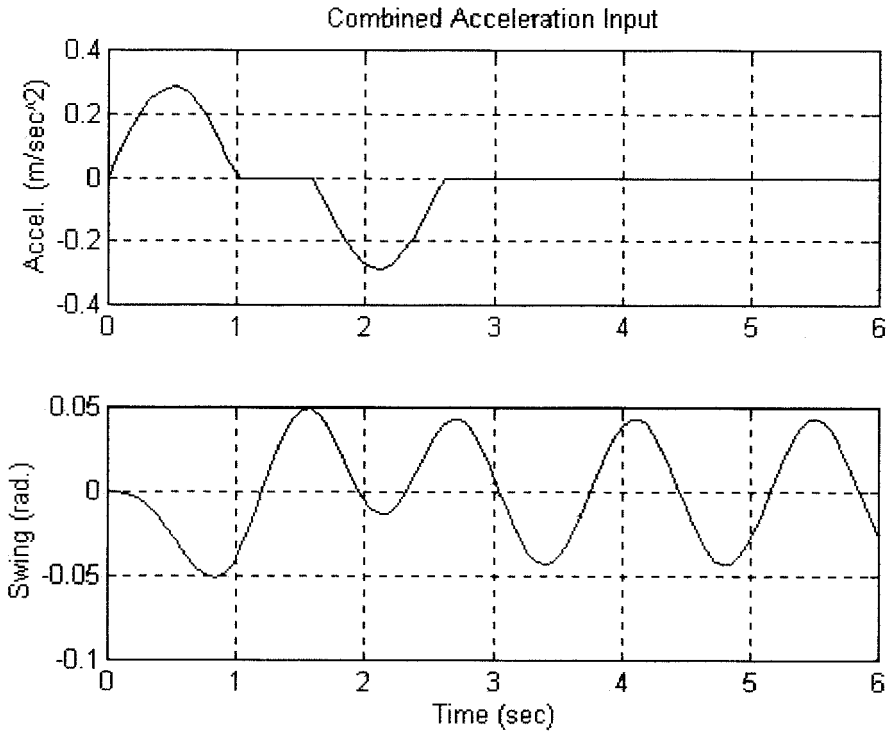

Fig. 6. Swinging response of the suspended object.

https://doi.org/10.1017/S0263574799001666 Published online by Cambridge University Press

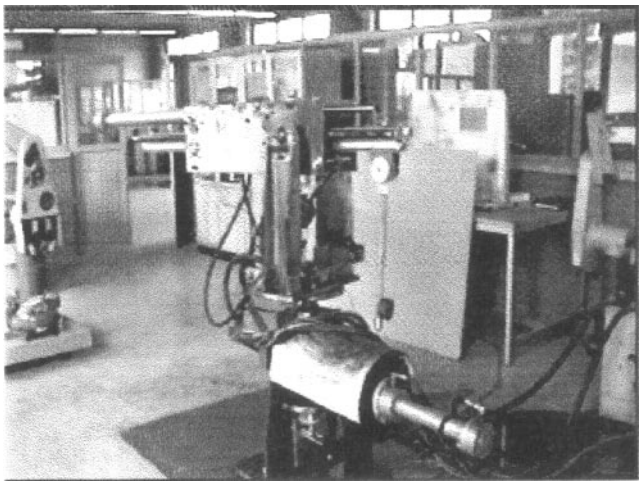

Fig. 7. Configuration of the robot manipulator and experimental set-up.

the sliding link comprising the dynamic load, a conductive plastic servo potentiometer to measure the swing of the suspended object, and hardware to control and command the manipulator, and read the potentiometer output. The manipulator links are controlled by Bosch regulator valves of 0811 404 028 type.[11]

The object of the experimental work has been to illustrate the effectiveness of the methods in preventing the swing of suspended objects. The translational link of the manipulator was kept parallel to the ground and was given the trajectories proposed in Section 3.

4.1 Experimental Results

Two sets of experimens have been conducted. The first set is for the method of constraining traveling time and the second is for that of adjusting the traveling time for each piece of a three-piece trajectory. In all the experimental results presented in this section, the top plot is the desired position input to the prismatic joint and the corresponding response, and the bottom plot is the recorded swing of the compound pendulum. Figure 8 shows the experimental result when the traveling time is calculated from Eq. 11, i.e., $\tau = \mathbf{2.8}$ seconds and the distance traveled is 0.292 m. This experimental result corresponds to the simulation result presented in Figure 2. Figure 9 shows the experimental result when the traveling time does not satisfy Eq. 11 i.e., $\tau = \mathbf{3.5}$ seconds. This experimental result corresponds to the simulation result shown in Figure 3. Note that there is a close correspondence between the experimental and simulation results.

The experimental result shown in Figure 10 is for the case when the traveling time for each piece of the three-piece trajectory are adjusted according to the theory presented in subsection 3.2. The data used for this result is the data in the simulation result depicted in Figure 5, i.e., $\tau_1 = \tau_3 = \mathbf{1.2}$ seconds, $\tau_2 = \mathbf{0.20}$ second, $\mathbf{X}_1 = \mathbf{X}_3 = \mathbf{0.125}$ m $\mathbf{X}_2 = \mathbf{0.042}$ m. Figure 11 shows the experimental result when the traveling times are not adjusted according to the theory. It is obtained for $\tau_1 = \tau_3 = \mathbf{1.0}$ second, $\tau_2 = \mathbf{0.600}$ second, $\mathbf{X}_1 = \mathbf{X}_3 = \mathbf{0.091}$ m and $\mathbf{X}_2 = \mathbf{0.110}$ m. Note that the total traveling time and the total distance traveled are unchanged. This experimental result corresponds to the simulation result presented in Figure 6.

Note that when the manipulator was commanded to follow a given trajectory without obeying the methods of adjusting the transportation time, the swing of the compound pendulum was exceptionally high, compare Figure 8 and Figure 9, and Figure 10 and Figure 11. Comparing Figure 2 and Figure 8, Figure 5 and Figure 10, it is clear that

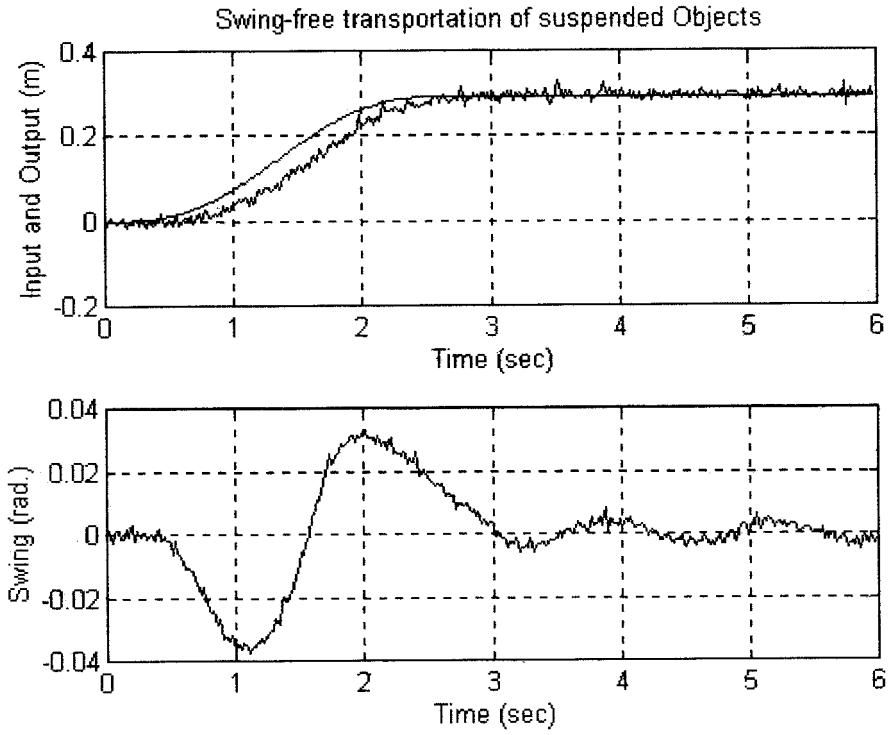

Fig. 8. Experimental swing-free response of the suspended object for $\tau = \mathbf{2.8}$ seconds.

https://doi.org/10.1017/S0263574799001666 Published online by Cambridge University Press

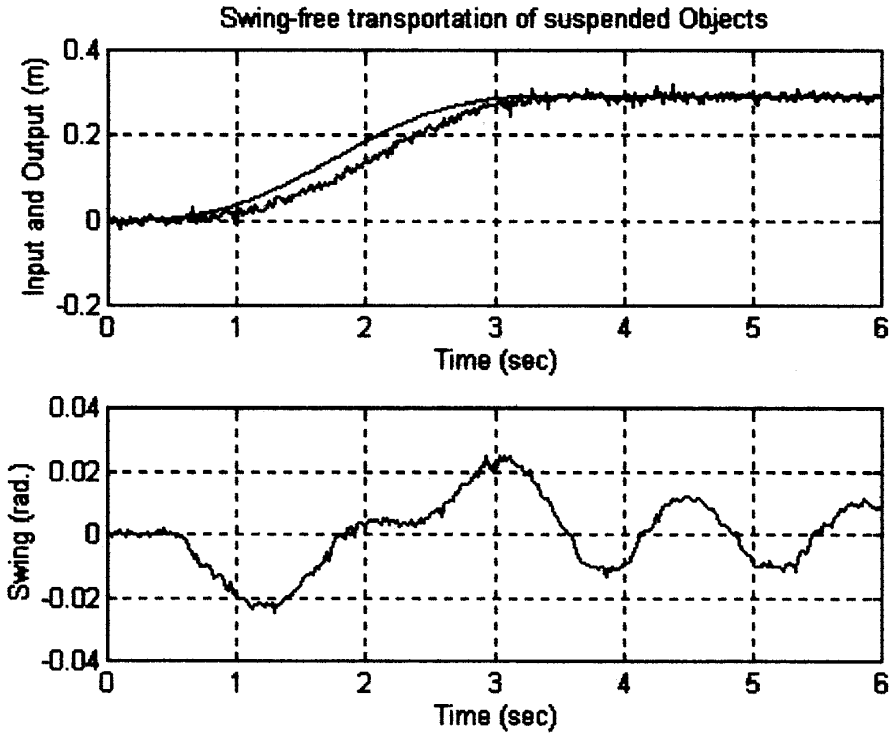

Fig. 9. Experimental swinging response of the suspended object for $\tau = \mathbf{3.5}$ seconds.

the methods perform as well on a real system as illustrated by simulation.

5. CONCLUSIONS

Two ways of eliminating the swing of suspended objects in transportation are presented. The simulation and experimental results reveal that it is possible to obtain a swing-free motion at the end of a move by employing the method of constraining the transportation time and the method of a three-piece combined trajectory. Any acceleration profile which satisfies the initial and final conditions of the move and preferably does not excite high frequency dynamics of the manipulator can be used as the acceleration of the suspension point. While limiting transportation time is not a preferred way to eliminate swing at the end of the move as it depends on the period of oscillation of the suspended object, the latter is a method which can find more popularity

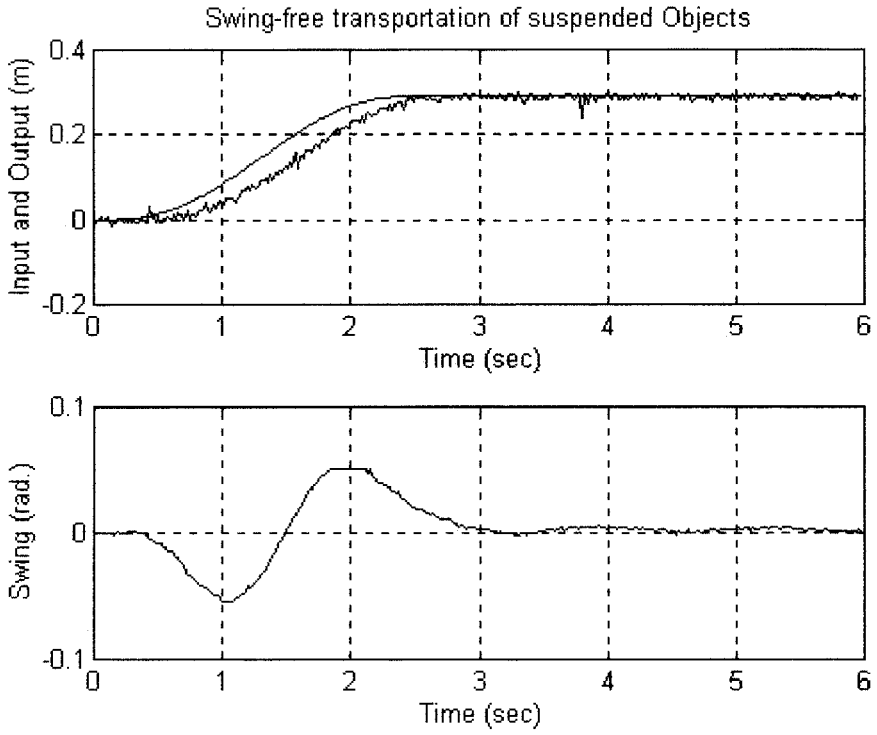

Fig. 10. Experimental swing-free response of the suspended object for a three-piece trajectory.

https://doi.org/10.1017/S0263574799001666 Published online by Cambridge University Press

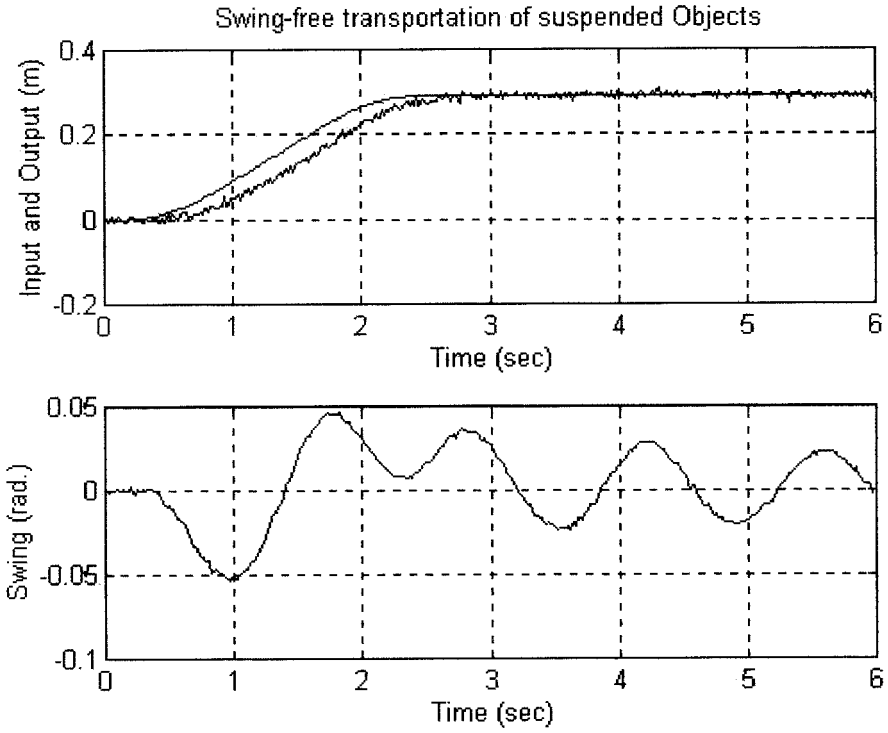

Fig. 11. Experimental swinging response of the suspended object for a three-piece trajectory.

and is valid for moves of any length in practice. This approach contributes to previously published work from the point of view of being simple and easy to implement, and can be considered as a versatile way to determine a trajectory resulting in no swing at the end of a move. We conclude that by properly programming the acceleration of the transporting device, a robot manipulator or a similar device such as a crane, a swing-free stop is obtainable.

References

1. G.P. Starr, "Swing-free transport of suspended objects with a path controlled robot manipulator", *ASME J. of Dyn. Syst. Meas., and Contr.*, **107**, 1, 97–100 (March, 1985).
2. D.R. Strip, "Swing-free transport of suspended objects: a general treatment", *IEEE Trans. on Robotics and Automation* **5**, No: 2, 234–236 (April, 1989).
3. W.E. Singhose and N.C. Singer, "Effects of Input Shaping on Two Dimensional Trajectory Following", *IEEE Transactions on Robotics and Automation* **12**, No: 6, 881–887 (December, 1996).
4. K.G. McConnell, and C.E. Bouton, "Noise and Vibration Control with Robust Vibration Suppression", *Sound and Vibration*, **31**, No: 6, 24–26 (June, 1997).
5. J.R. Jones, "A Comparison of Dynamic Performance of Tuned and Non-tuned Multiharmonic Cams", *2nd IFToMM International Symposium on Linkages and Computer Aided Design Methods*, Bucharest, Romania (1977) **Vol. III-2**, pp. 553–664.
6. N.C. Singer and W.P. Seering, "Preshaping Command Inputs to Reduce System Vibration", *ASME J. of Dynamic Systems, Measurement, and Control*, **112**, 76–82 (March, 1990).
7. S. Bayseç and J.R. Jones, "A Generalised Approach for the Modelling of Articulated Open Chain Planar Linkages", *Robotica*, **15**, Part 5, 523–531 (1997).
8. R.F. Steidel, *An introduction to Mechanical Vibrations*, 2nd ed. (John Wiley and Sons, 1979).
9. G. Lindfield and J. Penny, *Numerical Methods using MATLAB* (Ellis Horwood, 1995).
10. Y.F. Chen, *Mechanics and Design of Cam Mechanisms* (Pergamon Press, UK, 1982).
11. *Bosch Regulator Valves*, (Robert Bosch GmbH, Germany, 1987, 761302).

https://doi.org/10.1017/S0263574799001666 Published online by Cambridge University Press